

Measurements of evanescent wave in a sandwich Lamb wave sensor

Feng Li, Jean-François Manceau, Yihui Wu, and François Bastien

Citation: *Appl. Phys. Lett.* **93**, 174101 (2008); doi: 10.1063/1.3009562

View online: <http://dx.doi.org/10.1063/1.3009562>

View Table of Contents: <http://apl.aip.org/resource/1/APPLAB/v93/i17>

Published by the [American Institute of Physics](#).

Related Articles

Non-destructive imaging of an individual protein

Appl. Phys. Lett. **101**, 093701 (2012)

Ultrafast excited state dynamics of spirilloxanthin in solution and bound to core antenna complexes: Identification of the S and T1 states

JCP: BioChem. Phys. **6**, 08B610 (2012)

Ultrafast excited state dynamics of spirilloxanthin in solution and bound to core antenna complexes: Identification of the S* and T1 states

J. Chem. Phys. **137**, 064505 (2012)

Magneto-optic surface plasmon resonance optimum layers: Simulations for biological relevant refractive index changes

J. Appl. Phys. **112**, 034505 (2012)

Molecular-scale bio-sensing using armchair graphene

J. Appl. Phys. **112**, 014905 (2012)

Additional information on *Appl. Phys. Lett.*

Journal Homepage: <http://apl.aip.org/>

Journal Information: http://apl.aip.org/about/about_the_journal

Top downloads: http://apl.aip.org/features/most_downloaded

Information for Authors: <http://apl.aip.org/authors>

ADVERTISEMENT



HAVE YOU HEARD?

Employers hiring scientists
and engineers trust
physicstodayJOBS

<http://careers.physicstoday.org/post.cfm>



Measurements of evanescent wave in a sandwich Lamb wave sensor

Feng Li,¹ Jean-François Manceau,² Yihui Wu,^{3,a)} and François Bastien²

¹Changchun Institute of Optics, Fine Mechanics and Physics, Chinese Academy of Sciences, Changchun 130033, China; Graduate School of Chinese Academy of Sciences, Beijing 100039, China; and

²MN2S Department, FEMTO-ST Institute, 25044 Besançon, France

²MN2S Department, FEMTO-ST Institute, Université de Franche-Comté, CNRS, ENSMM, UTBM-32 avenue de l'Observatoire, 25044 Besançon, France

³Changchun Institute of Optics, Fine Mechanics and Physics, Chinese Academy of Sciences, Changchun 130033, China

(Received 25 April 2008; accepted 7 October 2008; published online 29 October 2008)

One method for evanescent wave measurement of the Lamb wave biosensor is proposed by putting another Lamb wave device above the first with the distance less than the evanescent field penetration depth in the liquid. The liquid layer is sandwiched with the two Lamb wave devices. The devices are interacted by an evanescent field; thus the evanescent wave can be studied. The mode is split by the interaction of the evanescent wave. The investigation of the evanescent field gives insight into acoustic biosensors and provides precise and multiparameter measurements. © 2008 American Institute of Physics. [DOI: 10.1063/1.3009562]

Within the fields of health care and environment control, there is an increasing demand for sensors able to detect low concentrations of particles such as molecular agents, warfare agents, or solid particles in gaseous or liquid samples.¹ The acoustic sensors, with their rapid response, portability, ease of use, and small size, are extremely useful for the analysis of both small and large molecules as well as whole cells interacting with an immobilized binding partner.^{2,3} The output signal provides information about the mass loading, intrinsic properties of bound materials, or viscoelastic effects such as structural rearrangements.

This letter focuses on the use of acoustic sensors using the propagation of one type of acoustic waves (Lamb wave sensor or flexural plate wave sensor). People pay more attention to the first antisymmetric mode (A_0) of the Lamb wave sensor because theoretically its sensitivity can reach 200–1000 g⁻¹ cm². The sensor has a phase velocity lower than the sound velocity of the loading liquid and the membrane functions as a wave guide while yielding no radiation losses in liquid despite the surface normal particle displacement.⁴ Therefore the A_0 mode is an excellent candidate for mass measurement for liquid biochemical reactions.

For the A_0 mode there are limitations to the applications. The biggest problem is that the signal is influenced dramatically by temperature variations. An on chip method which combines the A_0 mode and the first symmetric mode (S_0) to compensate for temperature was proposed by the authors.⁵ Since the S_0 mode vibration is almost tangential to the membrane, the wave barely penetrates the liquid. The mass sensitivity of the S_0 mode is even higher than that of the A_0 mode and the temperature responses of the A_0 and S_0 modes are opposite. The temperature may be compensated by combining these two modes without changing the device design.

Like the other acoustic sensors, the Lamb wave sensor is sensitive to many changes. The S_0 mode is mainly sensitive to the characteristics of the biolayer (thickness, density, viscoelasticity, temperature, etc.). The A_0 mode is not only sensitive to the characteristics of the biolayer; it is also sensitive

to the liquid characteristics (density and viscosity of liquid) due to its larger penetration depth. These parameters cannot be directly determined by the phases or amplitudes of these two modes. In fact, the distribution of the evanescent fields of the A_0 mode is influenced by these changes during the bioreaction. Therefore, the investigation of evanescent wave by the Lamb wave biosensor is significant for precise mass measurement and other parameters (such as thickness, temperature, viscosity, etc.). It has been suggested that it will allow the measurement of different molecules by adjusting the evanescent penetration.⁶

Unfortunately, due to the limitations on the sensors' size and the weak output signals, the intensity and distribution of the evanescent field for such devices are still not well known. Matula and Martin discussed the evanescent wave near the flexural metal plate ($\lambda=30$ mm) in liquid,⁷ but the bulky hydrophone was not suitable for the weak signal measurement of biosensors. Hongo and Nakamura introduced this kind of proximity sensor,⁸ however, their sensor could not directly measure the evanescent wave. Lloyd and Redwood predicted the existence of a guided mode of wave propagation in solid-fluid-solid trilayers.⁹ Thirty years later Hassan and Nagy measured these modes by laser interferometer.¹⁰ The evanescent field in the liquid has yet to be investigated.

In this letter, a device is presented to detect the evanescent field by coupling two Lamb wave devices with the distance less than the penetration depth of the evanescent field in the liquid. The Lamb wave dispersion and the evanescent field characteristics were studied by viewing the coupled output of these sensors.

When the device is loaded with liquid on one side, the theoretical penetration depth of the evanescent wave can be obtained by the following function:¹¹

$$\delta_e = \frac{\lambda}{2\pi} \sqrt{\frac{1}{1 - (\nu/\nu_l)^2}}, \quad (1)$$

where λ is the Lamb wave wavelength, ν is the Lamb wave phase velocity in the liquid, and ν_l is the sound speed in the liquid (de-ionized water). In our case, the evanescent wave theoretical penetration depth inside the water was 66 μ m.

^{a)}Electronic mail: yihuiwu@ciomp.ac.cn.

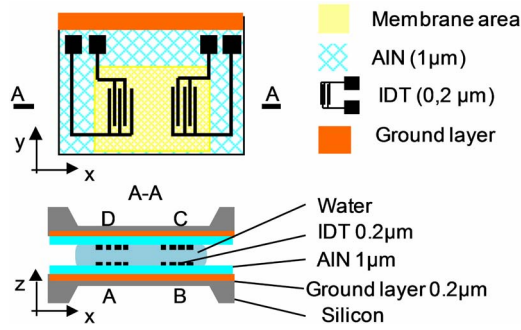


FIG. 1. (Color online) The setup of the sandwich Lamb wave device.

By attaching another Lamb wave sensor, as described, one liquid layer is sandwiched by the two Lamb wave sensors. The sensors interact with the evanescent field in liquid. The evanescent wave formed can be measured.

The Lamb wave devices in the experiments were fabricated by clean room facilities. The thickness of the membrane is $18 \mu\text{m}$ and its dimensions are $8000 \times 8000 \mu\text{m}^2$; two pairs of interdigital transducers (IDTs) were built on a $1 \mu\text{m}$ piezoelectric aluminum nitride (AIN) layer with a spatial period of $400 \mu\text{m}$. One pair of IDT is connected with the output of a gain-phase analyzer and excites the Lamb waves on the membrane; the Lamb waves propagate on the membrane and are transformed to an electrical signal by another IDT. The electrical signal is measured via the input of the gain-phase analyzer.

The experimental setup for the evanescent wave distribution measurement is shown in Fig. 1. Instead of measuring the Lamb wave directly at the output of the IDT as normal, the evanescent wave field distribution was measured by coupling the sensors' output. The two Lamb wave sensors were fixed on two different three-freedom precision stages as shown in Fig. 2. The upper Lamb wave sensor can be adjusted along the X , Y , or Z axis. The de-ionized water layer was kept between these sensors. The water layer thickness was changed by moving the upper sensor in the Z direction. Thus a sandwich Lamb wave sensor was constructed.

When the sensor is excited via port A, the acoustic waves propagate from A to B. At the same time the associated evanescent wave penetrates the liquid. If the upper sensor approaches δ_e , the acoustic energy is coupled into the upper Lamb wave sensor by the evanescent wave through the water. The output at port C represents the coupled response of the evanescent wave; alternately the output at port B represents the response of the guided wave in the membrane. By varying the distance between the two sensors and measuring

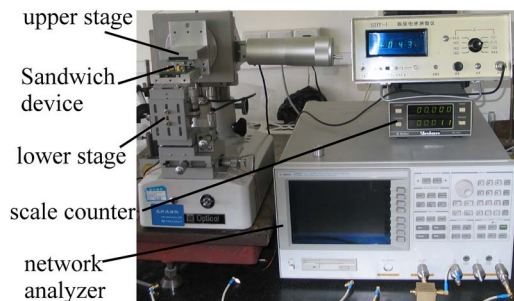
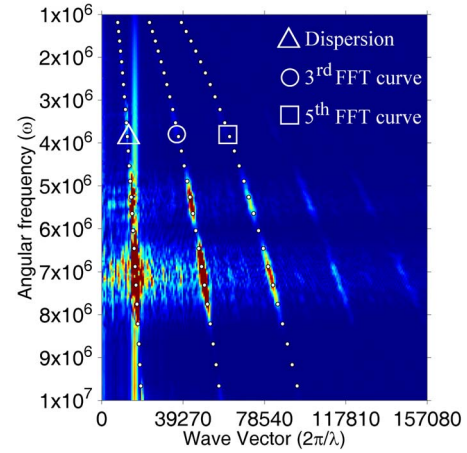


FIG. 2. (Color online) The experimental setup scheme for evanescent wave measurement.

FIG. 3. (Color online) Dispersion curve from FFT with the distance between two Lamb wave sensors of $100 \mu\text{m}$.

the output frequency response variation from the Agilent 4395A gain-phase analyzer at port C, the characteristics of the acoustic evanescent wave can be studied.

It should be noted that although the Lamb wave phase velocity is less than the sound velocity of water, near field sound emissions from the IDTs should not be neglected. The sound emissions will also be coupled into the upper sensor. Since the sound emissions propagate mainly in the Z -direction, by moving the upper sensor in the X direction, recording the signals and analyzing them by fast Fourier transforms (FFTs), the near field sound emissions can be efficiently filtered, producing the pure evanescent waves. In the experiment the upper sensor is moved along the X axis to a given Z position by stepping of $20 \mu\text{m}$ with a total movement of $9000 \mu\text{m}$. This is long enough to compare the Lamb wave wavelength ($400 \mu\text{m}$ here is).

While the upper sensor is moved along the X axis, both amplitudes and phases at C port were recorded. The disturbance of the Lamb wave due to the upper device is weak when the distance between two devices is much larger than the evanescent penetration depth of $66 \mu\text{m}$. In our case we chose $100 \mu\text{m}$. The dispersion curves using FFT calculations are shown in Fig. 3. The third and fifth spatial harmonics can also be found in Fig. 3. These effects are due to almost the nonpropagating spatial harmonics. In the dispersion curve, there is one line parallel with the frequency axis, which is due to the IDT effects of spatial periods and could be neglected during analysis.

The theoretical dispersion curves obtained from Eq. (2) were also shown in Fig. 3 by "0." This dispersion curve is given by the function

$$\omega = d \sqrt{\frac{E}{12\rho_{\text{Si}}}} \sqrt{\frac{\rho_{\text{Si}}d}{\rho_{\text{Si}}d + \rho_l \delta_e}} k^2, \quad (2)$$

where E is the Young modulus of silicon, d is the thickness of the membrane, ρ_{Si} and ρ_l are the density of the silicon and liquid, respectively, and k is the vector number. Comparing the theoretical and experimental results in Fig. 3, we see that the dispersion curves obtained from coupled sensor experiments agree with the theoretical calculation, which proves that the evanescent wave can be measured by this method.

However, when the distance between two devices is close to or less than the evanescent wave penetration depth,

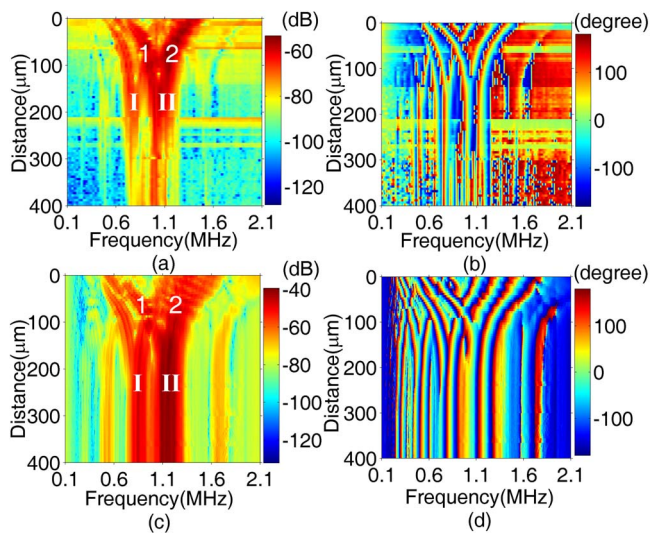


FIG. 4. (Color online) The amplitude and phase responses of the sandwich sensor variations showing distance changes. (a) is the amplitude variations with distance at C port; (b) is the phase variation with distance at C port; (c) is the amplitude variations at B port with distance; (d) is the phase variation at B port with distance.

the interactions between the two devices become stronger and the dispersion of Lamb wave in Fig. 3 distorts.

The responses variations at ports B and C of the sandwich Lamb wave sensor with an adjustment in the Z direction were represented in Fig. 4. Both the amplitudes and the phases show the splitting which appears when the distance becomes small, which shows that the two sensors are coupled in the region of the evanescent field and they begin to work as a sandwich sensor. The modes of this sensor are similar to the performance of two membranes separated by a layer of water which was described theoretically in Loyd and Redwood's paper⁹ and experimented with large aluminum plates and water by Hassan and Nagy.¹⁰

In Fig. 4, "1" is the symmetric mode of the sandwich Lamb wave sensor. As the two plates become closer, the amplitudes at both ports C and B become smaller. For the symmetric mode the movement of water is almost longitudinal; therefore for a small gap the liquid moves back and forth and is attenuated by viscosity; "2" is unsymmetric; the frequency becomes higher when the two membranes get closer due to the mass decreasing between two sensors. For this mode the amplitude at port C is increasing while that at port B is decreasing due to the energy of the lower sensor being

shared. This shows that the outputs of the sandwich sensor are highly influenced by the liquid thickness and its characteristics. There are two groups of response, "I" and "II," in Fig. 4 due to the fact that the node positions of the resonant membrane are not completely consistent with the position of IDT.

In summary compared with other acoustic sensors, such as Love wave sensors or quartz crystal microbalance (QCM), a unique feature of the Lamb wave sensor is that the deep evanescent field can be excited by the A_0 mode. One method for evanescent field detection was discussed in the letter and a sandwich Lamb wave sensor has been built.

The dispersion curves were obtained experimentally and it was proved that the evanescent wave is coupled into the upper device and the evanescent field is detected via this method. The sandwich sensor is very sensitive to the thickness variation due to the evanescent field interaction, which makes it possible to investigate the characteristics of the bilayer, such as its thickness, density, and viscosity, especially when it is combined with the S_0 and A_0 modes of the original Lamb wave sensors. This method gives insight into acoustic biosensors for the measurement. The density of liquid and the density and the thickness of the absorbed layer on the membrane can be evaluated, respectively, and allows precise multiparameter measurement.

The authors gratefully acknowledge Engineer L. Robert from FEMTO-ST in France for his AlN sputtering. The authors also wish to thank the French Embassy PHD Program, Hi-Tech R&D Program of China (863 Program Grant No. 2006AA04Z358) and Bureau of High-Tech R&D Chinese Academy of Sciences for the financial support.

¹L. Murphy, *Curr. Opin. Chem. Biol.* **10**, 177 (2006).

²B. Drafts, *IEEE Trans. Microwave Theory Tech.* **49**, 795 (2001).

³F. Herrmann, D. Hahn, and S. Buttgenbach, *Appl. Phys. Lett.* **74**, 22 (1999).

⁴B. Jacoby, J. Bastemeijer, and M. J. Vellekoop, *Sens. Actuators B* **82**, 83 (2000).

⁵F. Li, Y. Wu, J.-F. Manceau, and F. Bastien, *Appl. Phys. Lett.* **92**, 074101 (2008).

⁶T. M. A. Gronewold, *Anal. Chim. Acta* **603**, 119 (2007).

⁷T. J. Matula and P. L. Martin, *J. Acoust. Soc. Am.* **97**, 1389 (1995).

⁸S. Hongo and K. Nakamura, *IEEE Ultrasonics Symposium*, Toronto, Canada, 1997 (unpublished), p. 475.

⁹P. Lloyd and M. Redwood, *Acustica* **16**, 224 (1965/66).

¹⁰W. Hassan and P. B. Nagy, *J. Acoust. Soc. Am.* **102**, 3343 (1997).

¹¹S. W. Wenzel, B. A. Martin, and R. M. White, *Ultrasonics Symposium*, Chicago, IL, 1988 (unpublished), p. 536.